Spatio-Temporal Shorelines Change Model in Totok Bay Southeast Minahasa

J. C. Kumaat(✉), A. A. Tumengkol, X. E. Lobja, N. J. Sindua, and O. Watuseke

Faculty of Social Science, Manado State University, Manado, Indonesia
joykekumaat@unima.ac.id

Abstract. This study aims to analyze the rate of change in the shoreline and find out the back and forth of the coast in a certain period. Coastal areas play an important role in economic development, namely the transport and tourism industries. Unfortunately, the spatio-temporal variation of the shoreline is very dynamic and is of great concern due to the threat of erosion and accretion. This erosion mechanism is not only the result of natural processes (for example, wind, waves, currents and tides) but also human activity. In this study, the shoreline was considered the boundary between the continent and the sea. Due to the frequency of extreme events such as storm surges, floods, etc. especially in coastal areas in the past decades, scientists are increasingly interested in the study of shoreline dynamics. Satellite imagery used to interpret shoreline changes are Landsat 7 / Enhanced Thematic Mapper (ETM) imagery data path 112 row 59 dated September 11, 2001, Landsat 8 Operational Land Imager (OLI) imagery data path 112 row 59 dated October 22, 2013, and Landsat 8 Operational Land Imager (OLI) imagery data path 112 row 59 dated January 27, 2020, with a spatial resolution of 30 m. Analysis of changes in area was carried out intercropping between land and waters from all years. This method is carried out to find out the extent of the difference in the littoral regions of abrasion and accretion. This study used statistical data, namely NSM, EPR, and LRR with a distance along the shoreline of 10-m and a transect distance from the baseline of 30 m. The rate of abrasion and erosion in Totok Bay has a significant impact on the activities of its coastal communities, therefore handling protection of the shoreline needs to be carried out, such as by making sea walls or planting mangrove trees along the coast of Totok Bay.

Keyword: Spatio-temporal shorelines

1 Introduction

The world's population is almost about 60 percent inhabiting the coasts, human interest in inhabiting this place results in many problems faced such as changes in shorelines that almost hit all the coasts of the world [1]. Thus, coastal areas play an important role in economic development, namely the transport and tourism industries [2–5]. Unfortunately, the spatio-temporal variation of the shoreline is very dynamic and is of great concern due to the threat of erosion and accretion [6]. This erosion mechanism is not

R. Harold Elby Sendouw et al. (Eds.): UNICSSH 2022, ASSEHR 698, pp. 1825–1834, 2023.
https://doi.org/10.2991/978-2-494069-35-0_218

only the result of natural processes (for example, wind, waves, currents, and tides) but also human activity. Some research on shoreline changes has been conducted around the world, such as: [6–10], and to quantify any changes along the coastal area, detecting a shoreline defined as the intersection between the ocean and the earth's surface is an important step because it is used as a proxy for shoreline change [1, 11]. Remote sensing is a synoptic technique for analyzing the Earth based on efficiency, comfort, and cost. It is considered an effective option for extracting and monitoring the shoreline. Landsat imagery datasets are widely used in many studies since they were obtained freely from the Earth explorer platform of the United State Geological Survey (USGS) and provide reliable scientific information about the state of natural resources [12, 13].

Coastlines are sometimes assimilated to shoreline. However, there are some differences in nuance and complexity both in terms of practice and semantics [1], states that "the shoreline is the boundary between the land and the body of water. The term is considered synonymous with shoreline but is considered different, so the exact definition of shoreline is the line of contact between the average high waterline and the coast". According to [14, 16], "shoreline is defined as the edge of land at the limit of normal height" spring tides; subaerial land margins, often characterized by a boundary towards the sea of terrestrial vegetation. On the cliff beach, it is taken as the foot of the cliff in a high spring tidal level [17]. The shoreline is the water's edge, moving continuously as the tide rises and falls so that there is a low tide, a moderate shoreline, and a tidal shoreline [3]. The shoreline is the water's edge, moving to and continuously as the tide rises and falls so there is a low tide line, a medium shoreline, and a tidal shoreline [3, 18]. The shoreline thus moves constantly as tides rise and fall, while the shoreline is submerged only in exceptional circumstances (for example, during a surging storm) [18]. In this study, the shoreline was considered the boundary between land and sea [19, 20]. Due to the frequency of extreme events such as storm surges, floods, etc. especially in coastal areas in the past decades, scientists are increasingly interested in the study of shoreline dynamics. This study has two objectives, namely: measuring the rate of change in the shoreline and knowing the back and beachfront of the shoreline within a certain period.

2 Research Method

Satellite imagery used to interpret shoreline changes are Landsat 7 / Enhanced Thematic Mapper (ETM) imagery data path 112 row 59 dated September 11, 2001, Landsat 8 Operational Land Imager (OLI) imagery data path 112 row 59 dated October 22, 2013, and Landsat 8 Operational Land Imager (OLI) imagery data path 112 row 59 dated January 27, 2020, with a spatial resolution of 30 m. Landsat Satellite Imagery has the advantage of covering a large geographical area and has several bands with spectrum values suitable for the analysis of shoreline changes [21, 22]. Shoreline information is obtained by means of delineation carried out on a digital screen given the narrowness of the location where the digital study was conducted by identifying the difference in the boundary line between dry and wet areas [23]. Analysis of changes in area was carried out intercropping between land and waters from all years. This method is carried out in order to find out the extent of the difference in the littoral regions of abrasion and accretion [24]. Meanwhile, to determine the level of abrasion and accretion, transects

perpendicular to the deepest of the shoreline are used using the Digital Shoreline Analysis System (DSAS) [23, 25]–[27]. Calculations on the DSAS are based on the distance between the baseline and the entire shoreline. DSAS consists of several transects that can be determined according to coastal conditions [1, 28]. DSAS [1, 28, 29] automatically calculates statistical data for Shoreline Change Envelope (SCE), Net Shoreline Movement (NSM), End Point Rate (EPR), Linear Regression Rate (LRR), Weighted Linear regression (WLR), dan Least Median of Squares (LMS). This study used statistical data, namely NSM, EPR, and LRR with a distance along the shoreline of 10-m and a transect distance from the baseline of 30 m. The active data of EPR and LRR were then classified into 7 classes for abrasion and accretion. The classification calculation is based on the standard deviation and the average of the LRR and EPR. The statistical results and classification of EPR and LRR values are displayed in a map prepared using Arc GIS 10.7.1 software. Meanwhile, NSM data is used to see the accretion distance and abrasion changes that occur along the transect.

3 Results and Discussion

Landsat Satellite Imagery

Landsat imagery used in this study has been carried out *in the pre-processing* stage in *geometric correction*, *radiometric calibration*, *thermal atmospheric correction*, *dark object subtraction*, *layer stacking* and *region of interest*. There is a scene of data retrieval, namely for Landsat 7 ETM on September 11, 2001, and for Landsat 8 OLI on October 22, 201 and January 27, 2020, respectively (Fig. 1).

Shoreline Extraction

This *single Band 6 Threshold* analysis was carried out to separate and classify the pixel values of land and sea. This method is carried out by entering a minimum value of 0 for the sea and 1 for land from the shoreline pixel threshold value in the ENVI software tool build mask, for *Landsat* imagery in 2001,2013 and 2020 in the study entered a value of 0.009 in transitional pixels (Figs. 2 and 3).

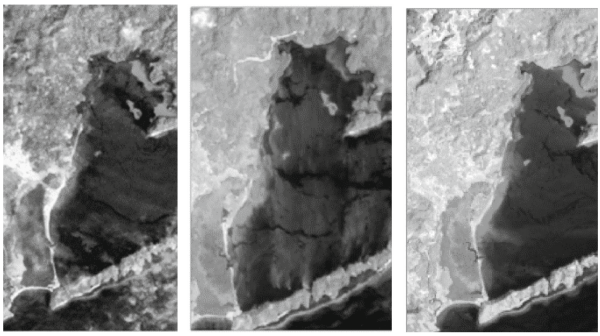

Landsat 7 ETM 11 September 2001 | Landsat 8 OLI 22 Oktober 2013 | Landsat 8 OLI 27 Januari 2020

Fig. 1. Landsat 7 ETM dan Landsat 8 OLI

A. Landsat 8 Band 6 Display In B. Single Band 6 Threshold Analysis

Fig. 2. Landsat 7 ETM dan Landsat OLI/TIRS

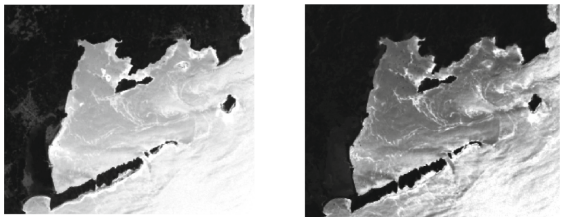

A. Band Ratio B3/B5 B. Band Ratio B3/b6

Fig. 3. Landsat 7 Band Ratio

A. Single Band 6 Threshold B. Rationing Band

Fig. 4. Landsat 7 ETM dan Landsat OLI/TIRS

Band Ratioing B3/B5 is carried out to separate objects The shoreline area is mostly surrounded by vegetation (Fig. 4.A), for shoreline areas that are not vegetated examples of sandy and mud shorelines used rationing B3/B6. So, the Band Ratioing technique is used for delineation of the shoreline. The Red band has its property of being absorbed by water, and only will be reflected in land. But on the other hand, in the Infrared, this work in adverse, i.e., the water reflects the spectrum more in comparison to land. So, the Band Red is divided by Band IR which provides the clear demarcation of water bodies and land. From the output, the shoreline was created in GIS (Fig. 4.B).

This study used a combination of the results of the multiplication of two Single Threshold Methods and Band Rationing as a shoreline delineation technique.

Figure 4 is the result of a delineation process of the shoreline in 2001, 2013 and 2020 from *derationed imagery*.

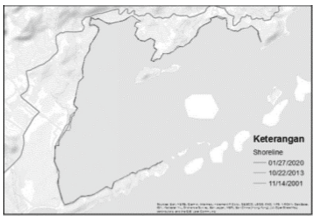

Fig. 5. Different Shoreline Landsat 7 ETM dan Landsat OLI

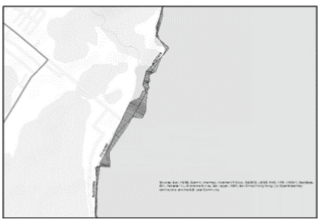

Fig. 6. Landsat 7 ETM dan Landsat OLI

In this study, the deliniation process of water and land boundaries from the imagery of Landsat 7 ETM and Landsat 8 OLI which has been rationed. Then continued with the rationing process that can obtain shoreline information by rolling the rationing results which are converted to vector format in the Arc Gis 10.7.1 software.

Figure 5 is the result of shoreline overlays in 2001, 2013 and 2020 the results of shoreline overlays will then be analyzed for changes with DSAS.

***Digital Shoreline Analysis System* (DSAS)**

Transect Line

The results of shoreline analysis management using the *Digital Shoreline Analysis System* (DSAS) are the distribution of transect lines with an interval of 10 m on the coast of Totok Bay and analyzed the calculation of changes.

Figure 6 shows the *transect* line formed using the *Digital Shoreline Analysis System* (DSAS) where the *transect* line is the entire coast of Totok Bay with the shoreline from 2001 to 2020, *transect* line in the form of 1758, so that *the transect is* resulting from processing with DSAS serves to calculate the analysis of changes in *the coordinate intersect* of the shoreline and *transect line.* The *transect* line that forms the entire coast of Totok Bay with the shoreline has coordinate values and distance differences. The difference in distance from the baseline calculation was used for the calculation, namely the shoreline in 2001.

Results of the 2001–2020 Shoreline Change Rate

Coastal Totok Bay, Southeast Minahasa Regency based on shoreline change analysis using the *Digital Shoreline Analysis System* (DSAS), The coast of Totok Bay has experienced a rate of change in the shoreline in certain areas during the period from 2001 to 2020 can be seen in Fig. 8. The results of the DSAS calculation for 19 years use the *Net Shoreline Movement* (NSM) and *End Point Rate* (EPR) methods where the NSM

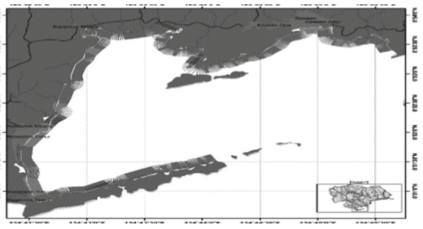

Fig. 7. Shoreline Change Rate Map 2001, 2013 and 2020

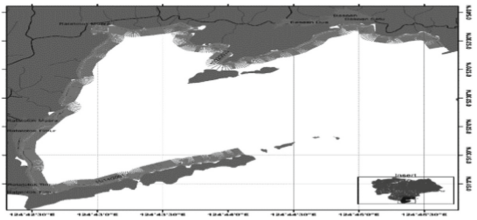

Fig. 8. Shoreline Change Rate Map 2001 – 2013

method for calculating the longest shoreline distance is 2001 with the latest shoreline, namely 2020, where the distance that is positive value (+) has the meaning of a forward shoreline and data that is negative (-) has the meaning of a backward shoreline. The EPR method is also used to calculate the rate of change in the shoreline each year, where data with a positive value (+) is accretion and data with a negative value (-) is abrasion. The coast of Totok Bay experiences the highest level of accretion with an average accretion rate of 0.75 m/year and an average distance of 13.93 m, while the one that experiences the highest abrasion rate with an average abrasion rate of -0.33 m / year and an average distance of change of -6.03 m. The location of the highest accretion occurs at the mouth of the river. Accretion is thought to be due to sedimentation that occurs at the mouth of the river and the addition of the area of mangrove vegetation as a coastal protector that has been planted at the mouth of the river and along the coast.

Results of the 2001–2013 Shoreline Change Rate

The shoreline in 2001–2013 (Fig.7), was mostly accretion based on the calculation results of the Digital Shoreline Analysis System (DSAS). The average accretion rate is the highest at 0.91 m/year in the coastal area of Totok Bay with an average distance of 10.89 m. The highest abrasion rate in the coastal area of Totok Bay with an average rate of -0.31 m/year and an average distance of change of -3.65 m. In 2001–2013 there were several development activities on the coast of Totok Bay such as Tempat Pelelangan Ikan (TPI) and the construction of a pier to support fishermen's activities around Totok Bay so that sedimentation occurred at the mouth of the river, DSAS calculations showed that the location experienced accretion. The occurrence of accretion can be caused by the existence of mangrove forests in coastal areas that have been widely converted into residential areas.

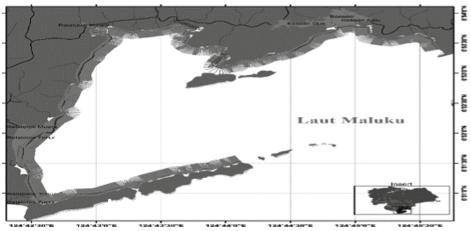

Fig. 9. Shoreline Change Rate Map 2013 – 2020

Results of the 2013–2020 Shoreline Change Rate

In 2013–2020, the shoreline of Totok Bay was mostly abrasion based on the results of DSAS calculations. The highest average accretion rate that has occurred in 2013–2020 was 0.97 m / year in the coastal area of Totok Bay located at the mouth of the river with an average distance of 6.05 m, while most coastal areas experienced the highest average abrasion rate of -1.13 m / year with an average distance of -7.09 m. An illustration of the 2013–2020 shoreline changes can be seen in Fig. 9. The pace of shoreline changes for 2013–2020 as we can see in Fig. 9 most of the shoreline of Totok Bay is abrasive. Based on the results of a survey from 2019 to date, namely 2020, that with the increase in the number of people in coastal areas, many mangroves forest lands have been converted into settlements so that the direction of the coming waves affects the rate of change in the shoreline.

Based on the results of this study, the rate of change in the shoreline is caused by hydro-oceanographic factors that affect each other. Abrasion occurs due to the movement of ocean currents parallel to the coast, coastal parallel currents tend to abrasion because sediments move to be carried away by the coastal parallel currents. The direction of the current is influenced by the direction in which the waves come towards the coast with the waves that occur aroused by the wind, causing coastal erosion. In addition, the beaches at the study site included sloping and sandy so that once a large wave from the sea direction to the coast caused the beach to erode or abrasion. Accretion occurs at the mouth of the river caused by the transfer of sediment from the estuary or the direction of the sea, causing silting.

4 Conclusion

The results of the DSAS calculation in 2001 - 2020 showed the highest accretion with an average accretion rate of 0.75 m / year and an average distance of 13.93 m, while experiencing the highest abrasion with an average rate of -0.33 m / year and an average distance of change of -6.03 m. The rate of change in the shoreline in 2001 – 2013 based on DSAS calculations Most of them experienced accretion. The average accretion rate is the highest at 0.91 m / year with an average distance of 10.89-m and the highest abrasion rate with an average rate of -0.31 m / year with an average distance change of -3.65 m. The rate of change in the shoreline in 2013 – 2020 was mostly abrasive based on DSAS calculations. The average accretion rate is the highest at 0.97 m / year with an average distance of 6.05 m, while the highest abrasion rate is on average at

-1.13 m / year with an average distance of -7.09 m. The rate of abrasion and erosion in Totok Bay has a significant impact on the activities of its coastal communities, therefore handling protection of the shoreline needs to be carried out, such as by making sea walls or planting mangrove trees along the coast of Totok Bay.

Acknowledgments. Research and membership at Konvensi can be held with financial assistance from the Faculty of Social Science, Universitas Negeri Manado, Indonesia.

References

1. D. N. Quang, V. H. Ngan, H. S. Tam, N. T. Viet, N. X. Tinh, and H. Tanaka, "Long-term shoreline evolution using dsas technique: A case study of Quang Nam province, Vietnam," *J. Mar. Sci. Eng.*, vol. 9, no. 10, pp. 1–18, 2021, doi: https://doi.org/10.3390/jmse9101124.
2. J. Atayi *et al.*, "A STUDY ON THE SHORELINE CHANGES AND LAND USE / LAND COVER ALONG," *Int. Arch. Photogramm. Remote Sens. Spat. Inf. Sci.*, vol. XLVI, no. March, pp. 6–8, 2022.
3. M. Ramdhan, Y. Yulius, and N. Kholik, "Shoreline Change Dynamics using Digital Shoreline Analysis in Cemara Besar Island," *J. Segara*, vol. 16, no. 2, pp. 105–114, 2020, doi: https://doi.org/10.15578/segara.v16i2.8360.
4. I. Pouye, D. P. Adjoussi, J. A. Ndione, A. Sall, K. D. Adjaho, and M. L. A. Gomez, "Coastline Dynamics Analysis in Dakar Region, Senegal from 1990 to 2040," *Am. J. Clim. Chang.*, vol. 11, no. 02, pp. 23–36, 2022, doi: https://doi.org/10.4236/ajcc.2022.112002.
5. J. C. Kumaat, M. T. Lasut, and A. S. Wantasen, "Geographic Information System Applications for BeachTourism Area Determination in Bitung City," *J. Ilm. PLATAX*, 2017, doi: https://doi.org/10.35800/jip.5.1.2017.14968.
6. E. Gairin *et al.*, "Spatiotemporal trends of bora bora's shoreline classification and movement using high-resolution imagery from 1955 to 2019," *Remote Sens.*, vol. 13, no. 22, 2021, doi: https://doi.org/10.3390/rs13224692.
7. M. A. Marfai, R. Winastuti, A. Wicaksono, and B. W. Mutaqin, "Coastal morphodynamic analysis in Buleleng Regency, Bali—Indonesia," *Nat. Hazards*, vol. 111, no. 1, pp. 995–1017, 2022.https://doi.org/10.1007/s11069-021-05088-8
8. L. Natarajan *et al.*, "Shoreline changes over last five decades and predictions for 2030 and 2040: a case study from Cuddalore, southeast coast of India," *Earth Sci. Informatics*, vol. 14, no. 3, pp. 1315–1325, 2021, doi: https://doi.org/10.1007/s12145-021-00668-5.
9. F. Guerrera, M. Martín-Martín, M. Tramontana, B. Nimon, and K. E. Kpémoua, "Shoreline changes and coastal erosion: The case study of the coast of togo (bight of benin, west africa margin)," *Geosci.*, vol. 11, no. 2, pp. 1–21, 2021, doi: https://doi.org/10.3390/geosciences11020040.
10. S. Arjasakusuma, S. S. Kusuma, S. Saringatin, P. Wicaksono, B. W. Mutaqin, and R. Rafif, "Shoreline dynamics in East Java Province, Indonesia, from 2000 to 2019 using multi-sensor remote sensing data," *Land*, vol. 10, no. 2, pp. 1–17, 2021, doi: https://doi.org/10.3390/land10020100.
11. A. Irsadi, N. K. T. Martuti, M. Abdullah, and L. N. Hadiyanti, "Abrasion and Accretion Analysis in Demak, Indonesia Coastal for Mitigation and Environmental Adaptation," *Nat. Environ. Pollut. Technol.*, vol. 21, no. 2, pp. 633–641, 2022, doi: https://doi.org/10.46488/NEPT.2022.v21i02.022.
12. M. W. Mwaniki, M. S. Moeller, and G. Schellmann, "A comparison of Landsat 8 (OLI) and Landsat 7 (ETM+) in mapping geology and visualising lineaments: A case study of central region Kenya," *Int. Arch. Photogramm. Remote Sens. Spat. Inf. Sci. - ISPRS Arch.*, vol. 40, no. 7W3, pp. 897–903, 2015, doi: https://doi.org/10.5194/isprsarchives-XL-7-W3-897-2015.

13. P. Lemenkova, "ISO Cluster classifier by ArcGIS for unsupervised classification of the Landsat TM image of Reykjavík," *Bull. Nat. Sci. Res.*, vol. 11, no. 1, pp. 29–37, 2021, doi: https://doi.org/10.5937/bnsr11-30488.
14. C. W. Finkl, "Coastal classification: Systematic approaches to consider in the development of a comprehensive scheme," *J. Coast. Res.*, vol. 20, no. 1, pp. 166–213, 2004, doi: https://doi.org/10.2112/1551-5036(2004)20[166:ccsatc]2.0.co;2.
15. P. PIRAZZOLI, "Geomorphological Indicators," *Encycl. Quat. Sci.*, pp. 2974–2983, 2007, doi: https://doi.org/10.1016/b0-444-52747-8/00138-1.
16. T. Scott, G. Masselink, and P. Russell, "Morphodynamic characteristics and classification of beaches in England and Wales," *Mar. Geol.*, vol. 286, no. 1–4, pp. 1–20, 2011, doi: https://doi.org/10.1016/j.margeo.2011.04.004.
17. K. K. Basheer Ahammed and A. C. Pandey, "Assessment and prediction of shoreline change using multi-temporal satellite data and geostatistics: A case study on the eastern coast of India," *J. Water Clim. Chang.*, vol. 13, no. 3, pp. 1477–1493, 2022, doi: https://doi.org/10.2166/wcc.2022.270.
18. J. Bosboom and M. Stive, *Coastal Dynamics Open Textbook*, vol. 1. 2021. doi: https://doi.org/10.5074/T.2021.001.
19. M. Tendean, A. T. Moningkey, and J. C. Kumaat, "Pemanfaatan Data Hidro Oseanografi dan Batimetri Untuk Penataan Pantai Tatapaan, Minahasa Selatan," *J. Episentrum*, vol. 1, no. 1, p. 1, 2020, doi: https://doi.org/10.36412/jepst.v1i1.1803.
20. J. C. Kumaat, K. S. Andaria, and D. Maliangkay, "Analysis of Floating Net Cage Based on Geographic Information System in Lembeh Island," *IOP Conf. Ser. Mater. Sci. Eng.*, vol. 1125, no. 1, p. 012024, May 2021, doi: https://doi.org/10.1088/1757-899X/1125/1/012024.
21. H. Hall, "Machine learning and remote sensing applications to shoreline dynamics," *M.Sc Thesis, Dep. Geogr. Univ. Cambridge*, no. November, 2021.
22. A. Vali, S. Comai, and M. Matteucci, "Deep learning for land use and land cover classification based on hyperspectral and multispectral earth observation data: A review," *Remote Sens.*, vol. 12, no. 15, 2020, doi: https://doi.org/10.3390/RS12152495.
23. M. Esmail, W. Mahmod, and H. Fath, "Influence of Coastal Measures on Shoreline Kinematics Along Damietta coast Using Geospatial Tools," *IOP Conf. Ser. Earth Environ. Sci.*, vol. 151, no. 1, 2018, doi: https://doi.org/10.1088/1755-1315/151/1/012027.
24. T. D. T. Oyedotun, "Shoreline Geometry : DSAS as a Tool for Historical Trend Analysis," *Geomorphol. Tech. (online Ed.*, vol. 2, no. October, pp. 1–12, 2014.
25. A. O. Adejoke and Yahaya Usman Badaru, "Accuracy Assessment of Pixel-Based Image Classification Of," *Kwali Counc.*, vol. 4, no. 22, pp. 133–140, 2014.
26. R. K. Karina and R. Kurniawan, "Identifikasi Penggunaan Lahan Menggunakan Citra Satelit Landsat 8 Melalui Google Earth Engine," *Semin. Nas. Off. Stat.*, vol. 2020, no. 1, pp. 798–805, 2021, doi: https://doi.org/10.34123/semnasoffstat.v2020i1.514.
27. K. Mangor, N. K. Drønen, K. H. Kærgaard, and S. E. Kristensen, *Shoreline management guidelines*, no. April. 2017.
28. B. W. Mutaqin, "Shoreline changes analysis in kuwaru coastal area, yogyakarta, Indonesia: An application of the digital shoreline analysis system (DSAS)," *Int. J. Sustain. Dev. Plan.*, vol. 12, no. 7, pp. 1203–1214, 2017, doi: https://doi.org/10.2495/SDP-V12-N7-1203-1214.
29. Himmelstoss, E.A., Henderson, R.E., Kratzmann, M.G., Farris, A.S.: Digital Shoreline Analysis System (DSAS) Version 5.1 User Guide: U.S. Geological Survey Open-File Report 2021–1091. U.S. Geol. Surv., p. 104 (2021).